

Autologous mesenchymal stromal cells immobilized in plasma-based hydrogel for the repair of articular cartilage defects in a large animal model

Karel Berounský^{1,2}, Irena Vacková^{3*}, Lucie Vištejnová^{4,5}, Anna Malečková^{4,5}, Jiřina Havránková^{4,5}, Pavel Klein⁴, Yaroslav Kolinko^{4,5}, Yuriy Petrenko^{3,6}, Šimon Pražák³, Filip Hanák^{1,2}, Jaromír Přidal^{1,2}, Vojtěch Havlas^{1,2}

¹Motol University Hospital, V Úvalu 84, Prague 150 06, Czech Republic

²Second Faculty of Medicine, Charles University, V Úvalu 84, Prague 150 06, Czech Republic

³Institute of Physiology, Czech Academy of Science, Vídeňská 1083, Prague 142 00, Czech Republic

⁴Charles University, Medical Faculty in Pilsen, Biomedical Center, Alej Svobody 76, Pilsen 323 00, Czech Republic

⁵Charles University, Medical Faculty in Pilsen, Department of Histology and Embryology, Alej Svobody 76, Pilsen 323 00, Czech Republic

⁶Institute of Experimental Medicine, Czech Academy of Science, Vídeňská 1083, Prague 142 00, Czech Republic

Corresponding author: Irena Vacková, Laboratory of Biomaterials and Tissue Engineering, Institute of Physiology of the Czech Academy of Sciences, Prague, Czech Republic. E-mail: irena.vackova@fgu.cas.cz

Short title: MSCs anchored in 3D scaffold for the cartilage repair

Summary

The treatment of cartilage defects in trauma injuries and degenerative diseases represents a challenge for orthopaedists. Advanced mesenchymal stromal cell (MSC)-based therapies are currently of interest for the repair of damaged cartilage. However, an approved system for MSC delivery and maintenance in the defect is still missing. This study aimed to evaluate the effect of autologous porcine bone marrow MSCs anchored in a commercially available polyglycolic acid-hyaluronan scaffold (Chondrotissue®) using autologous blood plasma-based hydrogel in the repair of osteochondral defects in a large animal model. The osteochondral defects were induced in twenty-four minipigs with terminated skeletal growth. Eight animals were left untreated, eight were treated with Chondrotissue® and eight received Chondrotissue® loaded with MSCs. The animals were terminated 90 days after surgery. Macroscopically, the untreated defects were filled with newly formed tissue to a greater extent than in the other groups. The histological evaluations showed that the defects treated with Chondrotissue® and Chondrotissue® loaded with pBMSCs contained a higher amount of hyaline cartilage and a lower amount of connective tissue, while untreated defects contained a higher amount of connective tissue and a lower amount of hyaline cartilage. In addition, undifferentiated connective tissue was observed at the edges of defects receiving Chondrotissue® loaded with MSCs, which may indicate the extracellular matrix production by transplanted MSCs. The immunological analysis of the blood samples revealed no immune response activation by MSCs application. This study demonstrated the successful and safe immobilization of MSCs in commercially available scaffolds and defect sites for cartilage defect repair.

Keywords: Bone marrow mesenchymal stromal cells, Scaffold, Osteochondral defect, Minipig, Implantation.

Introduction

Articular cartilage defects are a major cause of disability worldwide, affecting more than 22% of adults older than 40 years [1]. The self-regeneration capacity of cartilage tissue is limited due to the terminal degree of chondrocyte differentiation and poor tissue vascularization. The cartilage defects cause pain, bone deformities, joint swelling, and may lead to further degenerative joint diseases like osteoarthritis [2]. Despite the reported successes in the therapy of cartilage damage, only an insignificant number of treatment options may provide long-term improvement of cartilage tissue function [2-4]. New therapeutic strategies using multipotent mesenchymal stromal cells (MSCs) have been investigated for the treatment of cartilage defects [5,6]. MSCs are multipotent progenitor cells with prominent paracrine activity, immunomodulatory properties, and a capacity for multilineage differentiation [7]. Being successfully isolated from various adult and perinatal tissues (bone marrow, adipose tissue, skin, umbilical cord and others), their treatment potential for cartilage repair is the focus of many research and clinical studies [8-12].

Successful implantation and retention of MSCs in the defect is an important and non-negligible step in effective cell-based therapy. The use of a 3D scaffold may improve the therapeutic outcome by providing support for the implanted cells, enabling their incorporation into the surrounding tissue and/or the migration of the host tissue cells into the implant [13]. There have been several medical device scaffolds certified for the restoration of osteochondral defects in human medicine available on the market. The influence of 3D scaffolds on the restoration of cartilage defects is currently the subject of research [13-15]. Chondrotissue® (BioTissue AG, Zurich, Switzerland) is one of the commercially available scaffolds certified for the treatment of osteochondral defects in human medicine. The cell-free application of the Chondrotissue® graft has been shown to improve the quality and formation of reparative tissue, compared to the microfracture technique applied alone [16]. It has also been successfully used as a scaffold for autologous MSC implantation [17].

The efficient immobilization of viable cells within the scaffold may play a crucial role in the overall therapeutic effect. The fast immobilization of cells within the scaffold in the surgery room using hydrogel formulations can be considered the method of choice for ensuring the safety and reproducibility of the study.

Among the clinically acceptable hydrogels which can be used for the localized delivery of the cells, fibrin-/fibrinogen-based biomaterials are the most applied due to confirmed biocompatibility, safety, and natural origin [18]. The double-component products based on fibrinogen and thrombin are widely applied as tissue sealants, glues, or adhesives. However, their direct use for cell immobilization is challenging due to an extremely fast coagulation rate and significant stiffness of the obtained gels, which may lead to the reduction of cellular viability. As a natural autologous alternative to tissue sealants, the use of the mixture based on blood plasma (containing fibrinogen) and serum from the same patient (the source of natural thrombin) can be applied in clinical medicine and prepared in the operation hall immediately prior to use. In the presence of CaCl₂, such mixtures form a hydrogel in situ and have confirmed biocompatibility with both cells and the patient.

The safety of the autologous bone marrow MSCs implantation in Chondrotissue® scaffolds and plasma-based hydrogel was recently confirmed in a phase I/II clinical study [19]. However, a deep histological examination of the healing processes following the MSC-based graft implantation is needed to fully understand the therapeutic effects of implanted MSCs. Such histological studies are challenging to conduct in humans. Therefore, establishing a suitable large animal model and recapitulating the treatment conditions is required. Additionally, these models will serve for the further development of cell-based therapies using allogeneic MSCs that represent great opportunities for regenerative medicine as ready-to-use therapeutics.

The aim of this study was to evaluate the potential of autologous bone marrow MSCs immobilized in the Chondrotissue® scaffold by autologous blood plasma-based hydrogel in the repair of osteochondral defects. The adult minipig was used as the preclinical model to enable the histological evaluation of newly formed tissue in the defect.

Methods

Design of the experiment

Twenty-four minipigs (miniature Minnesota-based breed) with completed bone maturation at the age of 9 - 10 months, weighing 55 ± 5 kilograms, were included in the experiment. The animals were divided into one experimental and two control groups, with eight minipigs in each group. In all animals, the cartilage in the area of the medial femoral condyle of the left knee was artificially damaged. The induced osteochondral defects were either left without any treatment (group A), filled with Chondrotissue® combined with blood plasma-based hydrogel without pBMSCs (group B), or filled with Chondrotissue® enriched by pBMSCs isolated from the bone marrow of each individual animal and blood plasma-based hydrogel (group C). After 90 days, the entire knee condyles were explanted, and macroscopic evaluation and histological analyses were performed to determine and compare the results of the individual treatment group. The animals originated from the colony of the Institute of Animal Science in Kostelec nad Orlicí, Czech Republic. All the experimental procedures were approved by the Advisory Committee for Animal Welfare of the Ministry of Education of the Czech Republic (approval ID MSMT_12048_2019_5) and conducted under the supervision of the Advisory Committee for Animal Welfare of the Faculty of Medicine of the Charles University in Pilsen. The animals received standard care according to the EU Directive 2010/63/EU.

Isolation, culture, and characterization of autologous pBMSCs

pBMSCs were isolated from each of the 8 animals included in experimental group C. Three months before the experiment, bone marrow was collected from the femoral bone of each animal by a puncture with a sterile Ben biopsy needle (S. A. B. Impex, s.r.o., Bedřichovice, Czech Republic) and immediately transferred into 50 ml tubes (TPP) containing heparin (B Braun, Melsungen, Germany). Aspiration was performed under general anaesthesia and according to standard surgical procedure. pBMSCs were isolated as reported previously [20]. After isolation, pBMSCs on the second passage were cryo-preserved in liquid nitrogen (0.5 – 1.0 x 10⁶ cells/cryotube) for further use.

To confirm the purity of the pBMSCs intended for transplantations, their immunophenotypic profile (clusters of differentiations CD90, CD29, CD44, CD45 and major histocompatibility complex MHC II) and the

ability to differentiate into adipocytes, osteoblasts, and chondrocytes was determined according to our previous study [21].

Preparation of autologous blood plasma-based hydrogel for pBMSCs immobilization inside the scaffold

Four days before surgery, the stored pBMSCs were thawed and seeded at 10,000 cells per cm² into the 75cm² cell culture flasks (Techno Plastic Products, TPP, Trasadingen, Switzerland). At the time of operation, blood samples were collected from each animal, and the autologous serum and plasma were prepared for each animal (centrifugation 2000 x g, 10 min). At the same time, the pBMSCs were harvested and counted. To anchor the cells inside the scaffold, the cells were immobilized with an autologous blood plasma-based hydrogel prepared with minor modifications according to our previous studies [22,23]. Briefly, for group C, approximately 2.5 x 10⁶ cells were mixed with 90 µl of autologous plasma, and after transport from the lab to the operating room, cells with plasma were aspirated into a syringe containing 7.5 µl of autologous serum and 2.5 µl 10% CaCl₂ (BB Pharma a.s., Prague, Czech Republic). The syringe was gently tapped several times, and the MSC suspension was immediately applied to the Chondrotissue[®] filling of the cartilage defect. For group B, the procedure was similar, but the addition of cells was omitted. The gelation of the blood plasma-based hydrogel was completed within one to two minutes.

Surgical technique

After a premedication of Zoletil, Xylazine, and Atropine, general anaesthesia was maintained by administration of 1.0 – 2.0 % of isoflurane in O₂. The anaesthetic gases were administered via a human laryngeal mask using a standard veterinary anaesthesiologic apparatus equipped with an isoflurane evaporator. All surgical procedures were performed in aseptic conditions with sterilized surgical instruments. Subsequently, the left knee joint on the left hind leg was assessed through medial arthrotomy, the cartilage was exposed, and a circular osteochondral defect of standardized size (6mm in diameter, 2 mm deep to bleeding subchondral bone) was created using a custom-made tube osteotome in the load-bearing area of the medial femoral condyle (Figures 1A, B). In control group A, the defect was left without treatment. In control group B, the Chondrotissue[®] scaffold cut into a circular shape with the same diameter as the defect was inserted in the defect (Figure 1C). Subsequently, autologous blood plasma-based hydrogel was applied. In experimental group C, Chondrotissue[®] was inserted into the defect the same way as for control group B, and then the plasma-based hydrogel containing autologous plasma and serum with 10% CaCl₂ and autologous pBMSCs was applied on the surface of the scaffold (Figure 1D). The hydrogel soaked into the Chondrotissue[®] scaffold and solidified within about 1 or 2 minutes. The joint capsule, subcutaneous tissue, and skin were sutured, and a liquid Novikov dressing was applied to the wound to reduce the risk of wound complications.

After the surgery, the animals were observed in the intensive care unit for 12 hours and then transferred back to pens. Immediate weight-bearing and a full range of motion were allowed postoperatively. Trained animal keepers, supervised by a veterinarian, closely observed the animals. The minipigs were administered analgesia with Nalbuphine 0.25 mg/kg 8 hourly, and Tramadol 2 mg/kg together with Meloxicam 0.4 mg/kg during the following 3 days. 90 days after surgery, the minipigs were euthanized using intracardiac administration of thiopental and potassium chloride solution under general anaesthesia. Medial condyles with osteochondral defects were explanted, underwent a macroscopic evaluation and were fixed in a 4% formaldehyde solution for further histological analyses.

Macroscopic evaluation of explanted condyles

Immediately after the explantation of the medial condyles, all samples were evaluated by an experienced orthopaedist for the presence and visibility of the healed defects. The area of each healed defect underwent the macroscopic description.

Qualitative histological analysis

The explanted medial condyles were fixed in a 4% formaldehyde solution for 8 weeks and then decalcified in an ethylenediaminetetraacetic acid solution for 12 weeks. The samples were further decalcified for

8 weeks using Osteosens (Biognostrd.o.o., Zagreb, Croatia) and then immersed in 70% ethanol for 2 days. After dehydration and embedding in paraffin blocks, condyles were cut into 5 µm thick sections perpendicular to the long axis of the defect. The sections were stained by Verhoeff' shematoxylin/green trichrome and by periodic acid/Schiff reaction (PAS) plus alcian blue to distinguish connective tissue structures and acidic and neutral glycosaminoglycans forming the cartilage extracellular matrix. Digitalization of the slides was provided using the Olympus VS200 scanning system (Olympus, Japan). From the area of each histological section, which was blinded to the evaluator, the extent of healed tissue was determined, and the presence of hyaline cartilage, fibrous connective tissue, and undifferentiated connective tissue was qualitatively analyzed [24]. The samples were also analyzed for the presence of remnants of Chondrotissue® material.

Determination of inflammatory parameters in peripheral blood

Blood samples from the peripheral blood vessels were collected on days 0, 10 and 90 post-implantation to assess the safety and potential systemic inflammatory reaction in response to mesenchymal stem cell administration. The concentration of interleukins IL-1 beta, IL-4, IL-6, IL-8, IL-10, interferons alpha and gamma (IFN α and γ), tumour necrosis factor alpha (TNFα) and IL-12/IL-23p4 were measured using the Luminex assay (ProcartaPlex pig Cytokine, Chemokine Panel 9 plex, ThermoFisher Scientific, catalogue number EPX090-60829-901) according to the manufacturer's instructions using Luminex® xMAP Technology AtheNA Multi-Lyte® (ZEUS Scientific, Inc., NJ, USA). In ascending order, detection limits ranged from 1.14 to 6.91 for IFN α, IL-4, IL-10, IL-1 beta, IL-6, IFN γ and TNF α. The detection limits for IL-8 and IL-12/IL-23p4 were 24.9 and 72.1, respectively.

Statistical analysis

The minimum sample size for this experimental setup, estimated using G*Power software 3.7.1. [25], reached the value of 37 minipigs per group, assuming a medium effect size of 0.5 and a minimum power of 0.8. However, based on the previous experiments, it is not possible for economic and capacity reasons to have 111 animals in 3 groups. Only 8 animals were used in each group, which is in line with other animal studies [8,10,16,17], where 4 to 12 experimental animal models (rabbit, sheep, pig) were used per group. Moreover, the limited number of animals is in line with the 3Rs (three principles of welfare and protection of experimental animals - Replacement, Reduction and Refinement), which is the framework for experimental scientific work. The histological analysis did not provide any quantitative data requiring hypothesis testing.

Results

Isolation, culture and characterization of autologous pBMSCs

After isolation, porcine BMSCs adhered to the culture plastic and exhibited an elongated spindle-like morphology. The immunophenotypic profile of the cells confirmed the positivity of MSC markers CD90, CD29 and CD44 and the negativity of MHC II and hematopoietic cell marker CD45. The ability of cells to differentiate into adipocytes, osteoblasts, and chondrocytes was confirmed by histological staining using oil red "O", alizarin red and alcian blue (not shown).

Macroscopic evaluation of the defects from explanted condyles

The appearance of all explanted condyles was assessed macroscopically. The induced defect was still visible in all groups after 90 days, facilitating macroscopic evaluation and subsequent histological analysis (Figure 2A). The defect in control group A was macroscopically almost completely filled with newly formed tissue (Figure 2B). The transition between the newly formed tissue and the original cartilage was distinct, and the quality of the newly formed tissue was different and recognizable from the original hyaline cartilage. In contrast, in groups B and C, the newly formed tissue did not completely fill the induced defect (Figures 2C, D). An unfilled part remained in the middle of the defect in these groups. The subchondral bone was no longer visible in the centre of the defect, indicating the formation of new tissue in all parts of the defect. A transition between the original

cartilage and newly formed tissue was more clearly visible in groups B and C than in group A. There were no local adverse reactions seen in any of the specimens.

Qualitative histological analysis

The area of each histological section was examined in order to determine the extent of healed tissue. The area of newly formed tissue was qualitatively analyzed for the hyaline cartilage, fibrous connective tissue, and undifferentiated connective tissue. The results of qualitative analysis are summarized in Table 1. Defects without treatment (group A) were filled with a considerable amount of newly formed tissue without any visible empty space (Figures 3A, D). On the other hand, defects treated only with Chondrotissue® (group B) (Figures 3B, E) and Chondrotissue® loaded with pBMSCs (group C) (Figures 3C, F) were also filled with newly formed tissue. However, the unhealed empty space was still visible in the centre of the defects. The detailed qualitative analysis revealed that the newly formed tissue in the defects without any treatment (group A) was mostly composed of fibrous connective tissue and the hyaline cartilage was present to a lesser extent (Figure 4A, Table 1). On the contrary, a higher amount of hyaline cartilage and a lower amount of fibrous connective tissue was evident in both groups B and C treated only with Chondrotissue® (Figure 4B, Table 1) and pBMSC-loaded Chondrotissue® (Figure 4C, Table 1), respectively. Interestingly, the undifferentiated connective tissue (immature connective tissue, precursor of the hyaline cartilage) was observed at the interface of the defect and the new hyaline cartilage in some samples from the group treated with pBMSC-loaded Chondrotissue® (Figures 4C and 5). The remnants of Chondrotissue® material were observed only in two cases in group B.

Inflammatory response

The values of all monitored inflammatory parameters from the blood samples collected at all time intervals (0, 10, 90 days) were below the limits of detection of the given assay. The qualitative histological analysis did not reveal any chronic inflammation (immune cells infiltration or excessive connective tissue capsules) in the healing defects of all explanted samples.

Discussion

Several surgical methods have been introduced to treat damaged knee cartilage. These include pure debridement, bone marrow stimulating techniques (microfractures and drilling of the subchondral bone), mosaicplasty, autologous cultured chondrocyte implantation (ACI) or matrix-induced ACI (MACI), and filling the defect with an absorbable scaffold, usually combined with some of the other methods mentioned above [24]. However, most of these treatments lead to the ingrowth of fibrous connective tissue in the defect and do not ensure the formation of high-quality hyaline cartilage [26,27]. In the case of ACI and MACI, the patient is required to undergo multiple surgical procedures. Moreover, autologous chondrocytes are available in limited quantities, and their use is not suitable for treating large cartilage defects and older patients [11,27].

Due to the difficulties in obtaining autologous articular chondrocytes the use of autologous MSCs, derived mostly from bone marrow or adipose tissue, has been preferred for knee cartilage defect repair in both basic and clinical studies [9]. It has been shown that MSCs may synthesize the extracellular matrix, which closely mimics the healthy hyaline cartilage. Additionally, they secrete a cocktail of soluble factors, facilitating the regeneration and stimulating the growth of progenitor cells in situ [28]. A number of reports describe the use of autologous BMSCs as an effective and safe way of treating cartilage defects [29-31].

In a recent clinical study, published with our contribution, the implantation of BMSCs anchored in a 3D scaffold resulted in satisfactory short-to-medium-term therapeutic outcomes assessed by symptom relief (standardized scoring questionnaires) and structural changes (radiographs and magnetic resonance imaging) of the treated cartilage [19]. However, a histological follow-up of the healed defect was not performed.

In our study, we established the large animal model for a deep investigation of the regeneration process using histological evaluation. We aimed to evaluate the safety of intra-articular implantation of 3D graft, based on autologous MSCs for the treatment of artificially damaged knee cartilage as well as to establish the large animal model and operative procedures for the testing of future advanced therapy medicinal products in

preclinical settings. The experimental minipigs used in this study share many physiological similarities with humans. Their use in biomedical research offers several breeding, economic, and handling advantages compared to other large animal models [32].

In this study, we compared the efficacy of an implanted scaffold seeded with cultured autologous MSCs, the scaffold alone, or the defect without treatment on the healing of artificially created cartilage defects. As a 3D carrier, we used the resorbable polyglycolic acid-hyaluronan-based scaffold Chondrotissue[®], a commercially available 3D graft approved for human cartilage repair in cases of traumatic and degenerative changes of the synovial joints [14,15,19,33]. The safety of cell loaded Chondrotissue[®] implantation was confirmed by systemic blood testing for inflammatory factors at days 0, 10, and 90 after surgery, and the potential of the established 3D graft to stimulate new cartilaginous tissue formation was evaluated by macroscopic examination and qualitative histological assessment 90 days postoperatively. The monitoring of the inflammatory factors profile in the peripheral blood of the minipigs showed that the implantation of autologous MSCs was well-tolerated and did not cause any undesirable systemic inflammatory reactions or induce adverse effects and therefore was proved to be safe. The safety of implantation of autologous BMSCs in cartilage regenerative medicine has also been confirmed in other studies using animal models [17,34,35].

Macroscopic appearance and qualitative histological analysis revealed that all treated artificial osteochondral defects were filled with newly formed tissue. However, the quality of the newly formed tissue differed between the control and experimental groups. In particular, when observed macroscopically, the untreated control contained the most abundant amount of newly formed tissue. In contrast, histological analysis showed the fibrous nature of the formed matrix rather than cartilaginous. On the other hand, in the presence of Chondrotissue[®] scaffolds, a predominantly hyaline cartilaginous tissue was generated. The observed supportive role of scaffold implantation in the synthesis of new cartilage tissue during the healing of osteochondral defects is in line with other reported studies [16], confirming the potential of using this approach for further clinical application.

In addition, we applied blood plasma-based hydrogel to immobilize autologous BMSCs within the 3D Chondrotissue[®] scaffold. The use of blood plasma-based hydrogel improves the seeding efficiency and immobilization of cells within the 3D scaffold and inside the defect. Indeed, recent studies have confirmed that a 3D culture of MSCs in a fibrin-based hydrogel promotes cell proliferation, differentiation, and paracrine activity [36]. In addition, a significant increase in the secretion of various growth factors was observed in the 3D culture of MSCs inside the plasma-based hydrogels compared to standard monolayer conditions [22]. After implantation, the 3D MSC-based grafts possessed strong anti-inflammatory activity via the secretion of bioactive soluble molecules, additionally promoting hyaline cartilage healing [37]. In our study, the application of pBMSCs-loaded Chondrotissue[®] resulted in the generation of hyaline cartilaginous tissue in the treated defects, accompanied by the presence of undifferentiated connective tissue around the lesion. This observation suggests that MSCs may be involved in extracellular matrix (ECM) production at the site of the defect, which has been reported as a potential mechanism for cartilage regeneration after MSC implantation [38,39]. While the exact mechanism of MSCs in cell therapy and regenerative medicine is not fully elucidated, it is generally believed that their therapeutic activity is mediated primarily through a paracrine effect, in addition to ECM formation [40].

Conclusions

In the present study, we show the establishment of a relevant large animal model suitable for testing of tissue-engineered products combined with various types of cells. The study confirms that the use of autologous multipotent MSCs in a large animal model is safe. No local adverse reactions or elevation of specific inflammatory markers in the peripheral blood were observed at the selected intervals 0 - 90 days after surgery. In addition, morphological and histological screening of the healed defects 90 days postoperatively showed that both the scaffold without cells, as well as the scaffold loaded with mesenchymal stromal cells supported the cartilaginous regeneration of the osteochondral defects. Establishing the preclinical model is essential to test the safety of these cells before clinical trials in humans. In future experiments, we intend to use our experience with this

preclinical model in large-scale studies investigating the safety and efficacy of Wharton's jelly-derived allogeneic cells in treating osteochondral defects.

Conflict of Interest

There is no conflict of interest.

Acknowledgements

The study was supported by Ministry of Health, grant project No. NV19-06-00355, by the grant project MH CZ – DRO, Motol University Hospital, Prague, Czech Republic 00064203, by the Cooperation Program, research area MED/DIAG and research area SURG, and by SVV program number 260 651 provided by Charles University. Mr. Zac Kendell (First Faculty of Medicine, Charles University, Prague) is gratefully acknowledged for his language revision of the manuscript.

References

1. Cui A, Li H, Wang D, Zhong J, Chen Y, Lu H. Global, regional prevalence, incidence and risk factors of knee osteoarthritis in population-based studies. *E Clinical Medicine*. 2020;29-30:100587.
2. Robinson WH, Lepus CM, Wang Q, Raghu H, Mao R, Lindstrom TM, Sokolove J. Low-grade inflammation as a key mediator of the pathogenesis of osteoarthritis. *Nat Rev Rheumatol*. 2016;12(10):580-592.
3. Simon TM, Jackson DW. Articular Cartilage: Injury Pathways and Treatment Options. *Sports Med Arthrosc Rev*. 2018;26(1):31-39.
4. Lynch TS, Patel RM, Benedick A, Amin NH, Jones MH, Miniaci A. Systematic review of autogenous osteochondral transplant outcomes. *Arthroscopy* 2015;31(4):746-754.
5. Dewan AK, Gibson MA, Elisseeff JH, Trice ME. Evolution of autologous chondrocyte repair and comparison to other cartilage repair techniques. *Biomed Res Int*. 2014;2014:272481.
6. Hunziker EB. Articular cartilage repair: basic science and clinical progress. A review of the current status and prospects. *Osteoarthritis Cartilage*. 2002;10(6):432-463.
7. Petrenko Y, Vackova I, Kekulova K, Chudickova M, Koci Z, Turnovcova K, Kupcova Skalnikova H, Vodicka P, Kubinova S. A comparative analysis of multipotent mesenchymal stromal cells derived from different sources, with a focus on neuroregenerative potential. *SciRep*. 2020;10(1):4290.
8. Necas A, Plánka L, Srnec R, Crha M, Hlučilová J, Klíma J, Starý D, Kren L, Amler E, Vojtová L, Jančář J, Gál P. Quality of newly formed cartilaginous tissue in defects of articular surface after transplantation of mesenchymal stem cells in a composite scaffold based on collagen I with chitosan micro- and nanofibres. *Physiol Res*. 2010;59(4):605-614.
9. Pittenger MF, Discher DE, Péault BM, Phinney DG, Hare JM, Caplan AI. Mesenchymal stem cell perspective: cell biology to clinical progress. *NPJ Regen Med*. 2019;4:22.
10. Chang F, Ishii T, Yanai T, Mishima H, Akaogi H, Ogawa T, Ochiai N. Repair of large full-thickness articular cartilage defects by transplantation of autologous uncultured bone-marrow-derived mononuclear cells. *J Orthop Res* 2008;26(1):18-26.
11. Sadlik B, Jaroslowski G, Puzscharz M, Blasiak A, Oldak T, Gladysz D, Whyte GP. Cartilage Repair in the Knee Using Umbilical Cord Wharton's Jelly-Derived Mesenchymal Stem Cells Embedded Onto Collagen Scaffolding and Implanted Under Dry Arthroscopy. *Arthrosc Tech*. 2017;7(1):e57-e63.

12. Havlas V, Kos P, Jendelová P, Lesný P, Trč T, Syková E. Výsledky srovnání chondrogenní diferenciaci mezenchymálních kmenových buněk získaných z tukové tkáně s kultivovanými chondrocyty a mezenchymálními kmenovými buňkami z kostní dřeně [Comparison of chondrogenic differentiation of adipose tissue-derived mesenchymal stem cells with cultured chondrocytes and bone marrow mesenchymal stem cells]. *Acta Chir Orthop Traumatol Cech.* 2011;78(2):138-144.
13. Lee WY, Wang B. Cartilage repair by mesenchymal stem cells: Clinical trial update and perspectives. *J Orthop Translat.* 2017;9:76-88.
14. Andor B, Patrascu JM, Florescu S, Cojocar D, Sandesc M, Borcan F, Boruga O, Bolintineanu S. Comparison of different knee implants used on patients with osteoarthritis control study. *Mater Plast (Bucharest)* 2016; 53(1):119-125.
15. Glasbrenner J, Petersen W, Raschke MJ, Steiger M, Verdonk R, Castelli CC, Zappalà G, Fritschy D, Herbolt M. Matrix-Augmented Bone Marrow Stimulation With a Polyglycolic Acid Membrane With Hyaluronan vs Microfracture in Local Cartilage Defects of the Femoral Condyles: A Multicenter Randomized Controlled Trial. *Orthop J Sports Med.* 2020;8(5):2325967120922938.
16. Erggelet C, Endres M, Neumann K, Morawietz L, Ringe J, Haberstroh K, Sittinger M, Kaps C. Formation of cartilage repair tissue in articular cartilage defects pretreated with microfracture and covered with cell-free polymer-based implants. *J Orthop Res.* 2009;27(10):1353-1360.
17. Patrascu JM, Krüger JP, Böss HG, Ketzmar AK, Freymann U, Sittiger M, Notter M, Endres M, Kaps C. Polyglycolic acid-hyaluronan scaffolds loaded with bone marrow-derived mesenchymal stem cells show chondrogenic differentiation in vitro and cartilage repair in the rabbit model. *J Biomed Mater Res B Appl Biomater.* 2013;101(7):1310-1320.
18. Riedelová-Reicheltoová Z, Brynda E, Riedel T. Fibrin nanostructures for biomedical applications. *Physiol Res.* 2016;65(Suppl 2):S263-S272.
19. Neckar P, Potockova H, Branis J, Havlas V, Novotny T, Lykova D, Gujski J, Drahoradova I, Ruzickova K, Kaclova J, Skala P, Bauer PO. Treatment of knee cartilage by cultured stem cells and free dimensional scaffold: a phase I/IIa clinical trial. *Int Orthop.* 2022 Jul 19.
20. Vištejnová L, Liška V, Kumar A, Křečková J, Vyčítal O, Brůha J, Beneš J, Kolinko Y, Blassová T, Tonar Z, Brychtová M, Karlíková M, Racek J, Mírka H, Hošek P, Lysák D, Králíčková M. Mesenchymal Stromal Cell Therapy in Novel Porcine Model of Diffuse Liver Damage Induced by Repeated Biliary Obstruction. *Int J Mol Sci.* 2021;22(9):4304.
21. Horak J, Nalos L, Martinkova V, Tegl V, Vistejnova L, Kuncova J, Kohoutova M, Jarkovska D, Dolejsova M, Benes J, Stengl M, Matejovic M. Evaluation of Mesenchymal Stem Cell Therapy for Sepsis: A Randomized Controlled Porcine Study. *Front Immunol.* 2020;11:126.
22. Rogulska O, Tykhvynska O, Revenko O, Grischuk V, Mazur S, Volkova N, Vasyliiev R, Petrenko A, Petrenko Y. Novel Cryopreservation Approach Providing Off-the-Shelf Availability of Human Multipotent Mesenchymal Stromal Cells for Clinical Applications. *Stem Cells Int.* 2019;2019:4150690.
23. Vackova I, Vavrinova E, Musilkova J, Havlas V, Petrenko Y. *Polymers (Basel).* 2022;14(13):2553.
24. Filová E, Tonar Z, Lukášová V, Buzgo M, Litvinec A, Rampichová M, Beznoska J, Plencner M, Staffa A, Daňková J, Sural M, Chvojka J, Malečková A, Králíčková M, Amler E. Hydrogel Containing Anti-CD44-Labeled Microparticles, Guide Bone Tissue Formation in Osteochondral Defects in Rabbits. *Nanomaterials (Basel).* 2020;10(8):1504.
25. Faul F, Erdfelder E, Buchner A, Lang AG. Statistical power analyses using G*Power 3.1: tests for correlation and regression analyses. *Behav Res Methods.* 2009;41(4):1149-1160.

26. Welton KL, Logterman S, Bartley JH, Vidal AF, McCarty EC. Knee Cartilage Repair and Restoration: Common Problems and Solutions. *Clin Sports Med.* 2018;37(2):307-330.
27. Everhart JS, Campbell AB, Abouljoud MM, Kirven JC, Flanigan DC. Cost-efficacy of Knee Cartilage Defect Treatments in the United States. *Am J Sports Med.* 2020;48(1):242-251.
28. Dhinsa BS, Adesida AB. Current clinical therapies for cartilage repair, their limitation and the role of stem cells. *Curr Stem Cell Res Ther.* 2012;7(2):143-148.
29. Kristjánsson B, Honsawek S. Current perspectives in mesenchymal stem cell therapies for osteoarthritis. *Stem Cells Int.* 2014;2014:194318.
30. Yoshiya S, Dhawan A. Cartilage repair techniques in the knee: stem cell therapies. *Curr Rev Musculoskelet Med.* 2015;8(4):457-466.
31. Yamasaki S, Mera H, Itokazu M, Hashimoto Y, Wakitani S. Cartilage Repair With Autologous Bone Marrow Mesenchymal Stem Cell Transplantation: Review of Preclinical and Clinical Studies. *Cartilage.* 2014;5(4):196-202.
32. Vodicka P, Smetana K Jr, Dvorankova B, Emerick T, Xu YZ, Ourednik J, Ourednik V, Motlik J. The miniature pig as an animal model in biomedical research. *Ann N Y Acad Sci.* 2005;1049:161-171.
33. Zantop T, Petersen W. Arthroscopic implantation of a matrix to cover large chondral defect during microfracture. *Arthroscopy.* 2009;25(11):1354-1360.
34. Caminal M, Fonseca C, Peris D, Moll X, Rabanal RM, Barrachina J, Codina D, García F, Cairó JJ, Gòdia F, Pla A, Vives J. Use of a chronic model of articular cartilage and meniscal injury for the assessment of long-term effects after autologous mesenchymal stromal cell treatment in sheep. *N Biotechnol.* 2014;31(5):492-498.
35. Gugjoo MB, Fazili MR, Gayas MA, Ahmad RA, Dhama K. Animal mesenchymal stem cell research in cartilage regenerative medicine - a review. *Vet Q.* 2019;39(1):95-120.
36. Ortiz AC, Fideles SOM, Pomini KT, Reis CHB, Bueno CRS, Pereira ESBM, Rossi JO, Novais PC, Pilon JPG, Rosa Junior GM, Buchaim DV, Buchaim RL. Effects of Therapy with Fibrin Glue combined with Mesenchymal Stem Cells (MSCs) on Bone Regeneration: A Systematic Review. *Cells.* 2021;10(9):2323.
37. Le H, Xu W, Zhuang X, Chang F, Wang Y, Ding J. Mesenchymal stem cells for cartilage regeneration. *J Tissue Eng.* 2020;11:2041731420943839.
38. Ragelle H, Naba A, Larson BL, Zhou F, Prijjić M, Whittaker CA, Del Rosario A, Langer R, Hynes RO, Anderson DG. Comprehensive proteomic characterization of stem cell-derived extracellular matrices. *Biomaterials.* 2017;128:147-159.
39. Burk J, Sassmann A, Kasper C, Nimptsch A, Schubert S. Extracellular Matrix Synthesis and Remodeling by Mesenchymal Stromal Cells Is Context-Sensitive. *Int J Mol Sci.* 2022;23(3):1758.
40. Linero I, Chaparro O. Paracrine effect of mesenchymal stem cells derived from human adipose tissue in bone regeneration [published correction appears in *PLoS One.* 2015;10(3):e0119262]. *PLoS One.* 2014;9(9):e107001.

Tables

Table 1. The qualitative evaluation of the composition of newly formed tissue in osteochondral defects after 90 days of the healing. The process of healing of the osteochondral defect was compared between 3 groups – the empty defect without any treatment (group A), the group treated only with Chondrotissue® (group B), and the group treated with Chondrotissue® loaded with pBMSCs (group C). Each group consisted of 8 animals (N = 8). (+++) indicates the highest amount; (++) indicates the medium amount; (+) indicates the lowest amount; (n.i.) indicates that the defect was not included in the evaluation due to technical histological issues; (n.d.) indicates not detected.

<i>analysed parameters</i>	<i>new tissue in the defect</i>			<i>hyaline cartilage in new tissue</i>			<i>fibrous connective tissue in new tissue</i>			<i>undifferentiated connective tissue in new tissue</i>		
	<i>A</i>	<i>B</i>	<i>C</i>	<i>A</i>	<i>B</i>	<i>C</i>	<i>A</i>	<i>B</i>	<i>C</i>	<i>A</i>	<i>B</i>	<i>C</i>
<i>particular animals per group</i>	+++	++	++	+	+++	+++	+++	+	+	n.d.	n.d.	+
	+++	++	++	+	+++	+++	+++	+	+	n.d.	n.d.	+
	+++	++	++	+	+++	+++	+++	+	+	n.d.	n.d.	++
	+++	++	++	+	+++	+++	+++	+	+	n.d.	n.d.	+
	+++	n.i.	++	+	n.i.	+++	+++	n.i.	+	n.d.	n.i.	+
	+++	n.i.	++	+	n.i.	+++	+++	n.i.	+	n.d.	n.i.	++
	+++	++	++	+	+++	+++	+++	+	+	n.d.	n.d.	+
	+++	++	++	+	+++	+++	+++	+	+	n.d.	n.d.	+

Figure legends

Figure 1: Surgical technique of the animal experiment. A) medial approach to the knee joint with the creation of a standardized osteochondral defect with a custom-made osteotome; B) an artificially created osteochondral defect in the weight loading area of the medial condyle of the knee joint (6 millimetres diameter, 2 millimetres depth); C) defect filled with Chondrotissue® graft, cut in a circular shape corresponding to the diameter of the osteochondral lesion and; D) osteochondral defect filled with Chondrotissue® and covered with plasma-based hydrogel mixed with pBMSCs to cover the defect and anchor the cells inside the carrier.

Figure 2. Macroscopic evaluation of the osteochondral defects after 90 days following implantation. A) the medial condyle with visible osteochondral defect; B) defect without any treatment (group A); C) defect treated with Chondrotissue® alone (group B); D) defect treated with pBMSC-loaded Chondrotissue® (group C).

Figure 3. The whole area scans of histological sections throughout the osteochondral defects after 90 days of healing. The articular cartilage was observed around each sample. The healing defect (d) was approx. in the middle of the scan and was surrounded by bone tissue. A and D) defect without any treatment (group A); B and E) defect treated with Chondrotissue® without cells (group B); C and F) defect treated with pBMSCs-loaded Chondrotissue® (group C). A – C) stained by Verhoeff's hematoxylin/green trichrome (green is for cartilage and connective tissue, and purple is for bone tissue) and D – F) stained by PAS + alcian blue (violet is for connective tissue and bone and blue is for hyaline cartilage). Scale bars 5 mm.

Figure 4. Details of the healing process of osteochondral defects of cartilage after 90 days of healing. All sections were stained by PAS + alcian blue (violet is for connective tissue and bone and blue is for hyaline cartilage). A) defect without any treatment (group A); B) defect treated with Chondrotissue® without cells (group B); C) defect treated with pBMSCs-loaded Chondrotissue® (group C). d = defect; fCT = fibrous connective tissue; HC = hyaline cartilage; undifCT = undifferentiated connective tissue; B = bone. Scale bars 200 µm.

Figure 5. Detail of the undifferentiated connective tissue in sample from the defect treated with Chondrotissue® loaded with pBMSCs. The section is stained by PAS + alcian blue (violet is for undifferentiated connective tissue and blue is for hyaline cartilage). undifCT = undifferentiated connective tissue; HC = hyaline cartilage. Scale bar 200 µm.

Figures with legends

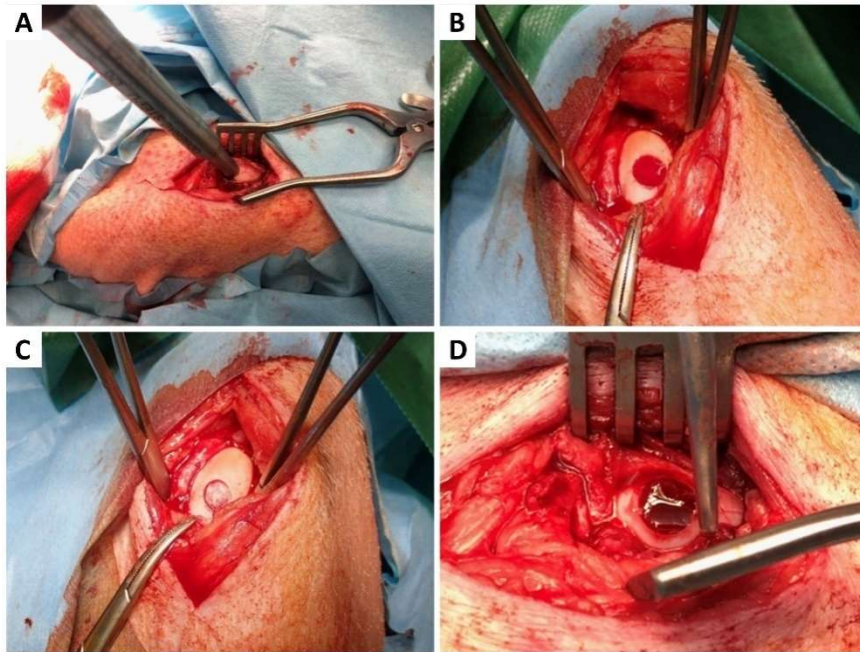


Figure 1: Surgical technique of the animal experiment. A) medial approach to the knee joint with the creation of a standardized osteochondral defect with a custom-made osteotome; B) an artificially created osteochondral defect in the weight loading area of the medial condyle of the knee joint (6 millimetres diameter, 2 millimetres depth); C) defect filled with Chondrotissue® graft, cut in a circular shape corresponding to the diameter of the osteochondral lesion and; D) osteochondral defect filled with Chondrotissue® and covered with plasma-based hydrogel mixed with pBMSCs to cover the defect and anchor the cells inside the carrier.

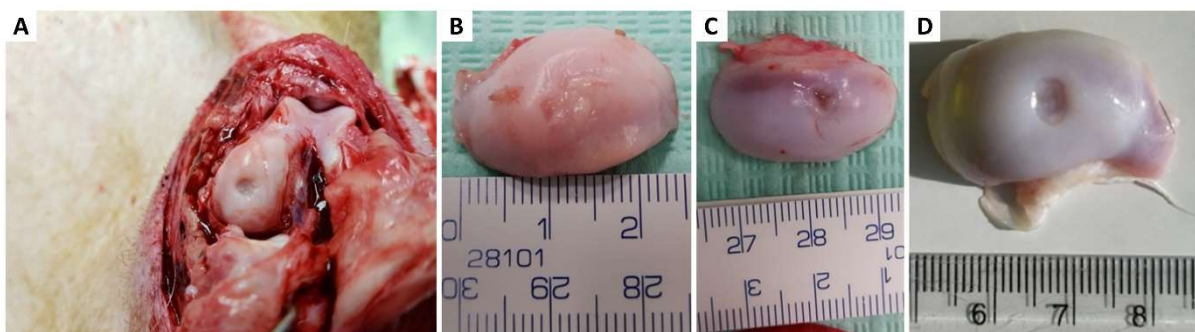


Figure 2. Macroscopic evaluation of the osteochondral defects after 90 days following implantation. A) the medial condyle with visible osteochondral defect; B) defect without any treatment (group A); C) defect treated with Chondrotissue® alone (group B); D) defect treated with pBMSC-loaded Chondrotissue® (group C).

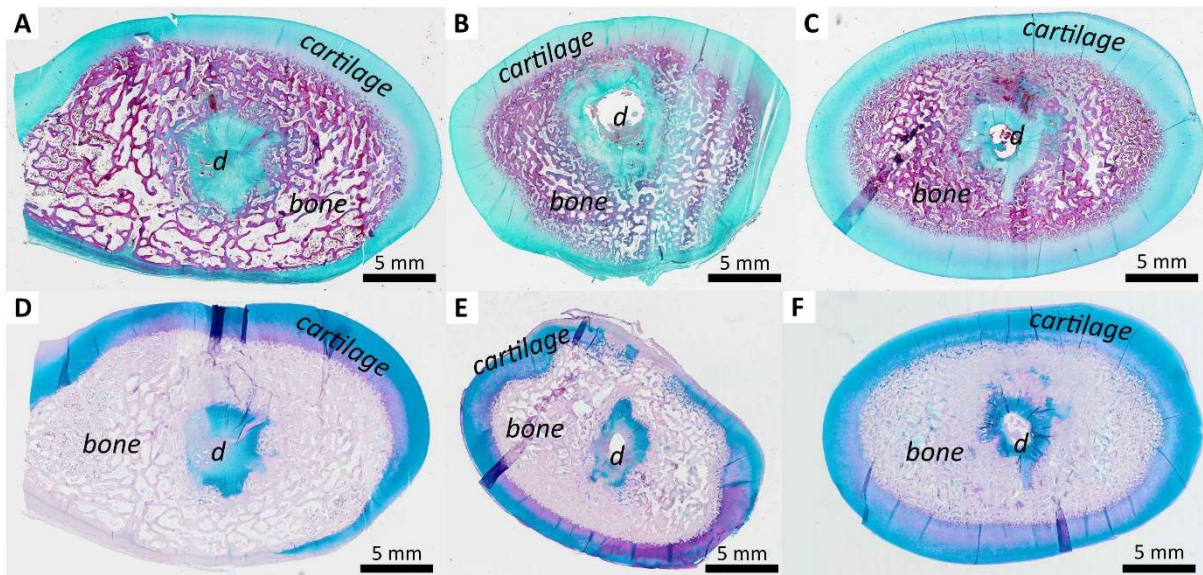


Figure 3. The whole area scans of histological sections throughout the osteochondral defects after 90 days of healing. The articular cartilage was observed around each sample. The healing defect (d) was approx. in the middle of the scan and was surrounded by bone tissue. A and D) defect without any treatment (group A); B and E) defect treated with Chondrotissue® without cells (group B); C and F) defect treated with pBMSCs-loaded Chondrotissue® (group C). A – C) stained by Verhoeff's hematoxylin/green trichrome (green is for cartilage and connective tissue, and purple is for bone tissue) and D – F) stained by PAS + alcian blue (violet is for connective tissue and bone and blue is for hyaline cartilage). Scale bars 5 mm.

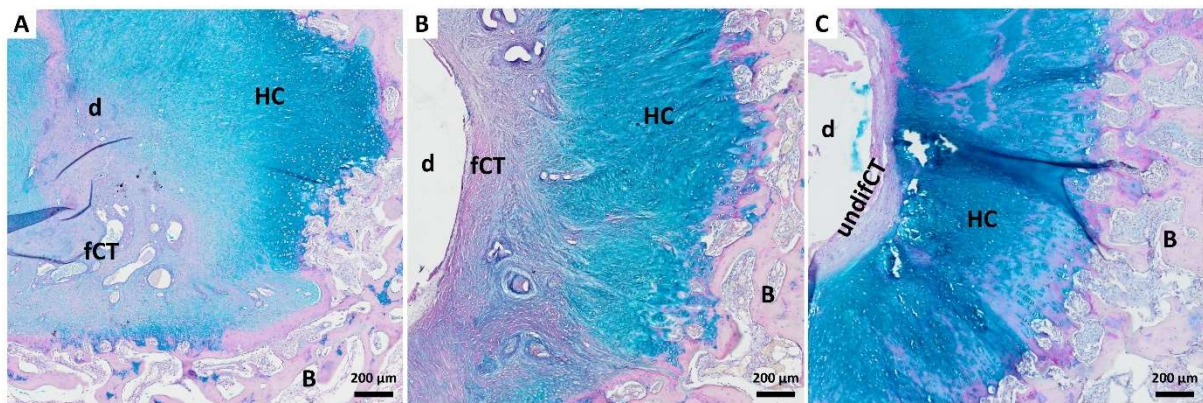


Figure 4. Details of the healing process of osteochondral defects of cartilage after 90 days of healing. All sections were stained by PAS + alcian blue (violet is for connective tissue and bone and blue is for hyaline cartilage). A) defect without any treatment (group A); B) defect treated with Chondrotissue® without cells (group B); C) defect treated with pBMSCs-loaded Chondrotissue® (group C). d = defect; fCT = fibrous connective tissue; HC = hyaline cartilage; undifCT = undifferentiated connective tissue; B = bone. Scale bars 200 µm.

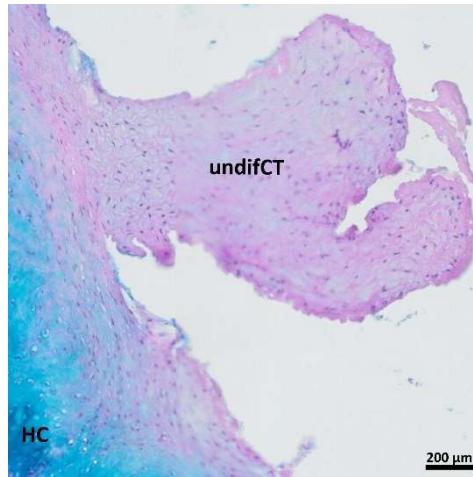


Figure 5. Detail of the undifferentiated connective tissue in sample from the defect treated with Chondrotissue® loaded with pBMSCs. The section is stained by PAS + alcian blue (violet is for undifferentiated connective tissue and blue is for hyaline cartilage). undifCT = undifferentiated connective tissue; HC = hyaline cartilage. Scale bar 200 μm.